

# INTERNATIONAL SOCIETY FOR SOIL MECHANICS AND GEOTECHNICAL ENGINEERING



*This paper was downloaded from the Online Library of the International Society for Soil Mechanics and Geotechnical Engineering (ISSMGE). The library is available here:*

<https://www.issmge.org/publications/online-library>

*This is an open-access database that archives thousands of papers published under the Auspices of the ISSMGE and maintained by the Innovation and Development Committee of ISSMGE.*

*The paper was published in the proceedings of the 20<sup>th</sup> International Conference on Soil Mechanics and Geotechnical Engineering and was edited by Mizanur Rahman and Mark Jaksa. The conference was held from May 1<sup>st</sup> to May 5<sup>th</sup> 2022 in Sydney, Australia.*

## A tomographic technique for measuring shear wave velocity in a drum centrifuge

Une technique tomographique pour mesurer la vitesse de l'onde de cisaillement dans une centrifugeuse à tambour

**Timothy Newson & Aly Ahmed**

*Department of Civil and Environmental Engineering, Western University, Canada, tnewson@eng.uwo.ca*

**Cristobal Lara & Giovanni Cascante**

*Department of Civil and Environmental Engineering, University of Waterloo, Canada*

**Edward Ginzel**

*Materials Research Institute, Waterloo, Ontario, Canada*

**ABSTRACT:** Elastic wave velocities are important parameters for characterizing soil properties for field sites and in laboratory specimens. The purpose of this paper is to describe the design and use of a miniaturized geophysics system for high resolution S-wave and P-wave velocity tomography in small-scale drum centrifuge models. This non-destructive technique will be used to infer changes in the static and dynamic properties of soils located in a centrifuge during experimental events and will provide vital information for later analysis. The system can use dry-point piezoceramic or bender-extender element transducers, interrogated with a ruggedized multi-channel ultrasonic in-flight instrument that can be used to simultaneously transmit and receive to (and from) linear and planar arrays of up to 32 geophysics sensors. A standard transducer calibration system is also described and pilot trials using ultrasonic dry point transducers were conducted to demonstrate the reproducibility and reduction in variability of the measurements for cylindrical soil proxy samples (porous filament 3D printed specimens).

**RÉSUMÉ :** Les vitesses des ondes élastiques sont des paramètres importants pour caractériser les propriétés du sol pour les sites de terrain et dans les échantillons de laboratoire. Le but de cet article est de décrire la conception et l'utilisation d'un système géophysique miniaturisé pour la tomographie de vitesse à ondes S et P à haute résolution dans des modèles de centrifugeuses à tambour à petite échelle. Cette technique non destructive sera utilisée pour déduire des changements dans les propriétés statiques et dynamiques des sols situés dans une centrifugeuse lors d'événements expérimentaux et fournira des informations vitales pour une analyse ultérieure. Le système peut utiliser des transducteurs à élément piézo-céramique à pointe sèche ou à élément bender-extender, interrogés avec un instrument de vol à ultrasons multicanaux robuste qui peut être utilisé pour transmettre et recevoir simultanément vers (et depuis) des réseaux linéaires et planaires de jusqu'à 32 géophysiques capteurs. Un système d'étalonnage de transducteur standard est également décrit et des essais pilotes utilisant des transducteurs à point sec à ultrasons ont été menés pour démontrer la reproductibilité et la réduction de la variabilité des mesures pour les échantillons de sol cylindriques (échantillons imprimés en 3D à filament poreux).

**KEYWORDS:** Shear wave velocity, Drum centrifuge, Signals, Calibration, Travel times

### 1 INTRODUCTION

Many of the theories used in geotechnical engineering have been developed using laboratory and field studies. Geotechnical centrifuge technology provides a method of reproducing full-scale ground stress profiles (and therefore their behaviour) within small-scale models in a controlled laboratory environment (Taylor, 1995). Scaled models have a distinct advantage over many other engineering approaches, since they provide greater control and reproducibility, and allow testing that cannot be conducted otherwise due to size, time, or safety constraints. Centrifuge modelling has provided significant and useful data relating to a range of geotechnical problems (Garnier et al., 2007). This has been aided in recent years by the development of improved soil deformation boundary visualization techniques, such as particle image velocimetry (e.g. White et al., 2001). Similar strides are now underway with the development of miniaturized geophysics systems that enable rapid non-contact investigation of the state of significant soil volumes in centrifuge models (e.g. Rammah et al., 2006).

Whilst the behaviour of dynamic stress waves, their reflection and attenuation have been the focus of many earthquake simulations in centrifuge modelling (e.g. Coe et al., 1985), less work has been conducted on other sources of elastic waves. Different excitation devices have been used for wave propagation analysis in centrifuge media (e.g. explosive sources,

vibratory loadings), and these vary in their ability to control the generated wave trains. The simulation of vibratory loads applied on the ground surface in a centrifuge was initially described by Cheney et al. (1990). Their system induced vertical cyclic loads on circular footings on dry sand. The energy transmitted to the ground from these footings traveled away from the source as a combination of compression, shear, and Rayleigh waves. Although the footings had built-in accelerometers, only the structural displacement with driving frequency was monitored and the experiments did not measure the actual wave propagation through the models.

The problem of ground vibration is now more common with increased development of urban structures and transport networks. Vibration generated by moving traffic propagates in the ground and into buildings. Davies (1994) investigated the feasibility of protecting buried structures from underground explosions using various forms of sub-surface barrier. Luong (1994) also examined the use of wave barriers to reduce vibration caused by traffic, vibratory machines, blast, shock, and impact loading. Itoh et al. (2005) studied ground vibration associated with high-speed trains using a single vibration source and a linear array of piezo-ceramic accelerometers. A number of researchers have investigated short (impulsive) wave trains using 'impactor' techniques (Abe et al., 1990; Luong, 1995). Semblat and Luong (1998) provided a more in depth understanding of wave propagation phenomena through a centrifuge model using

excitation from a dropping metal sphere. Wave reflections on model boundaries were taken into account and removed using homomorphic filtering. The wave propagation was investigated through dispersion laws and the generated spherical wave field was analysed assuming linear viscoelasticity, leading to a complete description of the wave propagation.

Bender elements are commonly used to estimate elastic shear and compression wave velocities in a range of laboratory soil specimens (Lee and Santamarina 2005). Testing systems are usually arranged as bender element 'couples' along the boundaries of the specimens. The elements consist of pairs of piezoceramic plates that are cross-sectionally polarized and bonded securely together. Recently, boundary bender element arrays have also been adopted for centrifuge test measurement of shear and compression wave velocity at different depths, in tomographic measurement systems and also as free elements within the soil body (e.g. Fu, 2004; Brandenburg et al, 2006; Rammah et al., 2006). These tomographic systems have typically utilized bender elements mounted on parallel planes, with multiple sets of source and receiver arrays. Since the bender elements generate relatively small amplitude shear waves and the amplitude of the received signals decrease with distance from the source, obtaining sufficient signal quality in centrifuge models is more difficult than in typical laboratory tests due to the increased distances. Researchers have tried to address this issue using higher voltages to excite the source bender elements and larger elements, to increase the measurable wave propagation distances, or have used sensitive signal conditioning hardware to maximize the received signals, whilst minimizing extraneous frequencies. Another issue for centrifuge-based systems is that vibration generated with the elements is transmitted through the supporting frame and mechanical vibrations of the centrifuge can also reach the receivers, affecting the detection of the intended wave fronts traveling through the soil mass. Several methods have been developed to filter these signals out of the data. To date, the effect of enhanced 'g' levels on the performance of bender elements has not been investigated and concerns relate to appropriate transducer selection and performance, transducer separation, frame characteristics, the selection of robust inversion algorithms to resolve images with limited information, and the development of adequate calibration procedures (Fernandez and Santamarina, 2003).

Multi-Channel Analysis of Surface Waves (MASW) is a non-destructive *in situ* test method that produces a near-surface shear wave velocity profile of the soil (Park et al., 1997). The method makes use of the dispersive nature of Rayleigh waves (Aki and Richards, 2002), where different wavelengths have different penetration depths and thus propagate with different velocity. A line of equally spaced seismographs, usually 24 or more over 2 to 200 m, is used to record the vertical acceleration produced by passive sources or an impulsive load (Park et al., 2007). The records are processed to obtain the dispersion curves from which the shear wave profile is reconstructed. MASW has also been investigated using 1g sandbox models (Kirlangic et al., 2015; Ali, 2015). The laboratory tests were conducted using different configurations of model and involved use of linear arrays of accelerometers as receivers, with different input sources. The results from these laboratory MASW tests show the frequency effects on the measurements due to the different sources used in this method. To date no centrifuge based MASW studies have been reported in the literature. Other researchers have also investigated the use of elastic wave measurements to identify large scale phenomena in soil bodies. Chen et al. (2019) investigated the effect of initiation of failure in a slope on the elastic wave velocities using a single vibration source and piezoelectric vibration sensors embedded through the models.

The purpose of this paper is to describe the design and use of a general miniaturized geophysics system for high resolution S-wave and P-wave velocity tomography for small-scale drum centrifuge models. This non-destructive technique will be used

to infer changes in the static and dynamic properties of soils located in the centrifuge during experimental events and will provide vital information for later analysis. The system is based on dry-point piezoceramic and bender-extend element arrays, and the paper describes the initial steps of development: concept, system design and calibration of the transducers.

## 2 METHODOLOGY

### 2.1 Overview of the Western drum centrifuge

The Western University (Ontario) recently commissioned a Broadbent 2.2 m drum centrifuge for scaled physical modeling of geotechnical processes and structures. The new facility has been supported by a \$5.4M grant from the Canada Foundation for Innovation Research Fund. The facility is located in a dedicated laboratory with a floor area of 300 m<sup>2</sup>, which includes space for the drum centrifuge and a control room, model/instrumentation preparation and testing, storage, image analysis and data processing. The centrifuge consists of a 360-degree drum channel 0.4 m deep and 0.7 m wide, with a diameter of 2.2 m, able to hold up to 3.5 tonnes of soil. The drum is mounted via a central shaft on a pedestal, which is powered by a 35 kW motor that creates a hyper-gravity environment up to 249g. Therefore the 867 g-tonne machine has one of the largest 'scaled-model' soil environments in the world; an equivalent of 13.3M m<sup>3</sup> of soil, i.e. a soil body approximately 80 m deep, with a plan area of 0.08 km<sup>2</sup> and a length of 0.7 km.

A centrally located tool-table system provides easy access to the spinning drum and is a structure mounted coaxially within the drum to which actuators and sensors can be fitted. The tool table has an independent secondary motor and can be brought to rest and held stationary while the drum is in-flight, allowing actuators and sensors to be worked on or changed without affecting the model test. The tool table can be accelerated back up to drum speed, locked to the drum and then accurately indexed at low-speed relative to the drum, to allow interaction with the model at any desired location. A three-axis robot is attached to the tool table that allows accurate positioning and load application in the X, Y and Z directions while stationary or in-flight. This enables site investigation tools, structural loading or instrumentation, etc. to interact with the model. The robot can be used to apply various loading (+/- 10 kN) or displacement (0-5 mm/s) control profiles to soil bodies or structures, such as monotonic, periodic, successive step or multiple cycles (see Figure 1).

Twin high-speed data acquisition systems for the drum environment and the tool-table are capable of simultaneous interrogation of 64 channels of data with additional on-board digitization, network acquisition and control. Computer controlled two axis in-flight placement/pouring is used for preparation of soil layers with controlled density and strength. A profile actuator permits the creation, changing and monitoring of model soil surfaces in-flight. A range of miniature instrumentation allows the measurement of stresses, forces and movements of soil sediments and structures in the models. Miniature site investigation devices comprise of a piezocone penetrometer and a shear vane. Additional tools are available for T-bar and plate penetrometer testing.

Of the 98 geotechnical centrifuge facilities in the world, the vast majority of these are in Japan (38) and the USA (21), with only four in Canada. All of the other Canadian facilities have fixed-beam machines and they reside in the University of Alberta, Queen's University, the University of New Brunswick and the C-Core research facility in St. John's Newfoundland, which is affiliated with Memorial University. The latter centrifuge facility is the only large geotechnical centrifuge, with a 5 m radius and a 220 g-tonne capacity. The C-Core machine has a large model box capacity (1m x 1m x 1.5m), which is well suited for certain classes of problem, particularly where large

amounts of instrumentation are required or the user is investigating structural ‘elements’ or smaller portions of an overall geotechnical system.

Of the remaining centrifuges in the world, only ten of these are ‘drum’ centrifuges and these are located in Japan, Brazil, Australia, UK, China, Switzerland and USA; the nearest being located at UC Davis in California. Drum centrifuges have advantages of being able to operate at higher ‘g’ levels, giving greater scaling gains and provide longer continuous lengths of soil. Hence drums can model long single geotechnical structures, e.g. a slope, pipeline or tailings dam, or can be used to simulate a long site with soil that has a common geological history, enabling comparison of different structures or replication of tests in the same material (see Figure 2). Due to their structural differences (compared to more typical fixed beam machines), drum centrifuges have far more lateral space available for instrumentation and actuators within the drum, but less space available in the centre of the centrifuge for data acquisition systems (although this is somewhat accommodated by the ability to quickly change devices in-flight). The tomographic system described in the next section of the paper has been designed with these constraints in mind.

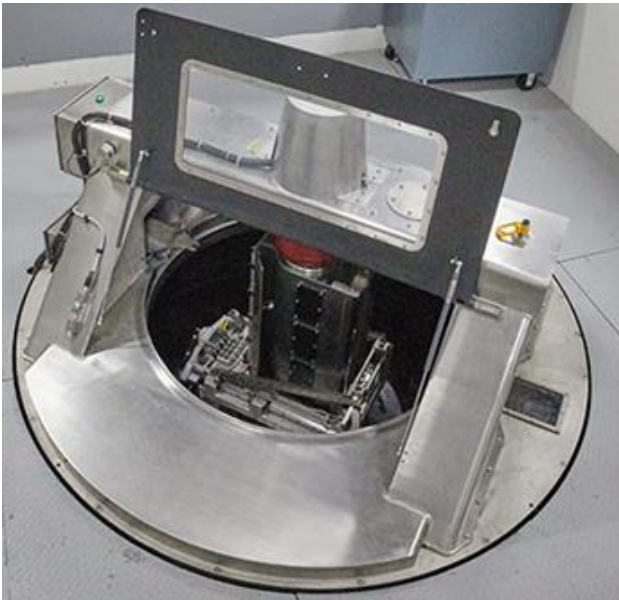


Figure 1. Western geotechnical drum centrifuge and 3D robot

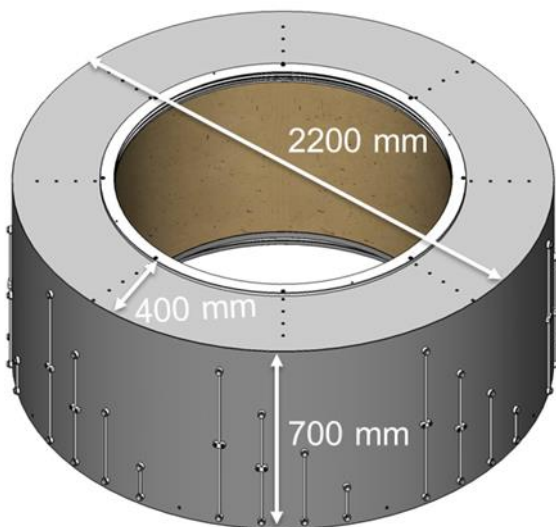


Figure 2. The 2.2 m diameter drum channel geometry

## 2.2 Overview of Tomographic System

Assessment of the condition of soils during scaled model testing using geophysical techniques is a critical step in the development of reliable methods for the prediction and evaluation of spatial stiffness, saturation and packing state variations. Geophysical tests provide non-destructive measurements from the surface and sub-surface of the soil body that reveal three-dimensional information about the sub-surface. This paper describes the development of a ruggedized multi-channel ultrasonic in-flight instrument that can be used for interrogating up to 32 geophysics sensors in the large Western 2.2 m geotechnical drum centrifuge. This system will enable linear and planar arrays generating and receiving shear and compression waves to visualize wave velocity distributions with tomographic inversion up to 100g. This non-destructive method will be used for monitoring changes of soil condition in scaled physical models during experiments. The development and optimization of the associated hardware and software for the centrifuge environment is discussed herein.

The assessment of soils during centrifuge testing will eventually be conducted using two high-resolution geotomography systems based on: (i) embedded lateral arrays of bender-extender element (BEE) transducers and (ii) multichannel analysis of surface waves (MASW) linear surface arrays of dry point piezo-ceramic (DPP) transducers. For brevity, only the DPP system will be described within this paper. The multi-channel pulsing and receiving system is housed in a curved ruggedized box (see Figure 3) that can sit on the edge of the drum environment and connects to the transducers through low noise cables with twin Lemo-00 ends.

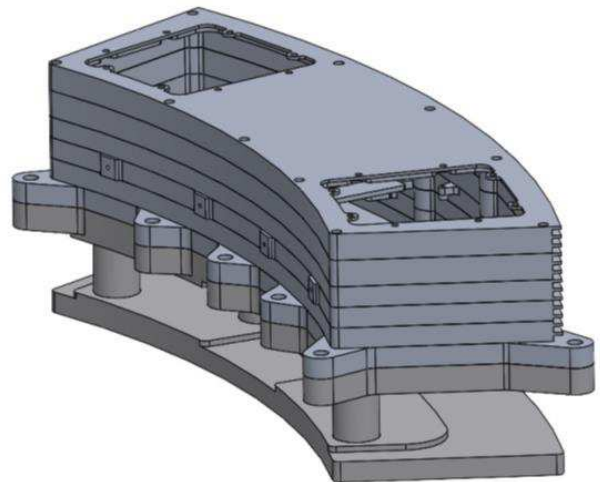


Figure 3. General schematic of the ruggedized multi-channel pulsing and receiving system.

The required parameters for the pulsing and receiving components of the system include:

- Pulse Shape - Square wave negative full-cycle and half cycle negative;
- Pulse Amplitude - Up to 400 V (full wave), 200 V negative half-wave;
- Signal Averaging - Up to 32 averages available;
- Gain Range - 90dB;
- Sampling Frequency - 16-Bit with capability to sample at 50, 25, 12.5 and 6.25 MHz;
- System Receiver Bandwidth - 5kHz to 2 MHz;
- Filtering - Broadband, High pass, Low pass and none;
- Max Points per A\_Scan - Up to 8000.



### 2.3 Calibration and Validation Exercises

All of the transducers that will be used in the centrifuge need to be appropriately characterized and calibrated. However, there is no standard or code regulating a consistent method to calibrate transducers for P-wave and S-wave velocity measurements (e.g. dry point or bender elements) for geotechnical testing. Calibration of the transducers requires a specimen of an appropriate size, shape and material with well-defined and uniform properties. The transducers need to be correctly coupled and aligned with the specimen to ensure effective transference of energy, reduce near field effects, prevent local alteration of the specimen and preserve the integrity of the transducer. Reproducibility of the calibration process and measurement outcomes is also important.



Figure 4. S1802 ultrasonic low-frequency dry point piezoceramic shear wave transducer

The transducers described in this paper are S1802 dry point piezoceramic (DPP) probes (manufactured by ACS International). Bender elements are bi-morphic with twin plates of different materials in a plastic protective coating, designed to work in direct contact with soft materials (soils). The DPP transducers (Figure 4) are also bi-morphic, but have the moving ends attached to an actuator that moves the ceramic wear tip (shown in red). The DPP transducers also incorporate a liquid damping substance that results in a very short oscillation time, creating relatively broadband pulses. The design concept for the transducer is to ensure that the size of the acoustic contact zone of the oscillating probe surface (with the surface of the test object) is many times smaller than the length of the ultrasound wave generated. The transducer has two piezo-elements and these allow control of the directivity of the wear tip oscillations. In-phase stimulation produces longitudinal oscillations of the wear tip and anti-phase stimulation creates shear oscillations. Phasing of the piezo-elements for modes of radiation (Tx) and reception (Rx) can be realized with an electric commutator built in to the case of the probe.

The transducers can generate both normal and tangential oscillation forces on the solid body's surface (Shevaldykin et al., 2003) and the transducer acts on the test object surface as a point oscillating force. The transducers have a nominal frequency of 50 kHz, a band width of 10 to 100 kHz and an operating temperature range of -20 to +50°C. The transducer shown in Figure 4 has dimensions (height x diameter) of 46 x 15 mm and a weight of 18 g. A sketch of the transducer and a graph of its frequency response is also shown in Figure 5. The oscillatory motion on the tip follows the left to right movement described with a double head arrow in Figure 5-a. The maximum excitation voltage for these transducers is 400 V.

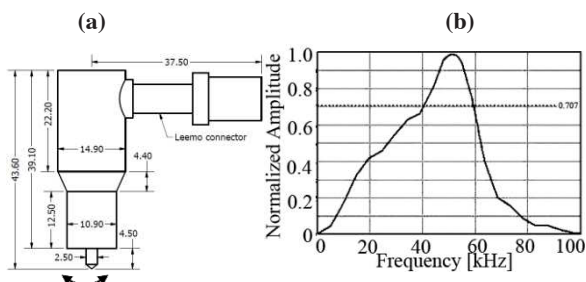


Figure 5. Dry point transducer specification. a) Transducer dimensions in mm, b) Frequency response

Figure 6 shows the transducer holder and specimen arrangement for the calibration of the DPP probes. As discussed previously, one problem characterizing the dry point transducers is guaranteeing that the coupling remains constant between tests, with the same contact pressure and the same orientation each time. Hence the test setup described herein was developed. The setup consists of two DPP holders, which are used to orientate and safely hold the sensors, whilst applying a standardized pressure to the sensor to push them against the test specimen, sitting between the two sensors. Each dry point transducer is therefore connected with a spring force (2.7 kg for these tests) to ensure reproducible test conditions for calibration.

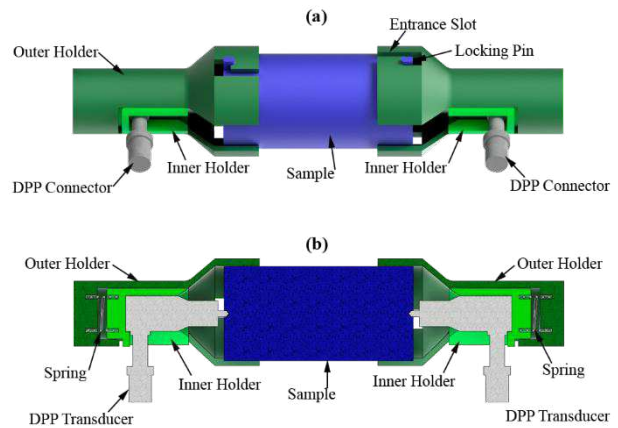


Figure 6 (a) DPP holders (dark green) and specimen (blue) linkages. (b) Cross-section through the system showing the DPP sensors (grey), internal fitment holders (light green), pressure spring location (black) and dry point sensor tips in contact with the specimen.

Previous researchers have calibrated similar transducers using tip-tip measurements or metallic specimens (Camacho-Tauta et al., 2012). To improve on these approaches, a stiff PLA (polylactic acid) engineering plastic specimen was formed using filament 3D printing. The advantage of this material is that it has similar elastic wave properties to soils and can be created with various infill densities and void patterns. For a 100 % infill cube, the compression mode velocities were found to be in the range of 2085-2156 m/s. For the tests described herein, the standard specimen was cylindrical with dimensions of 80 mm length and 40 mm diameter. The infill pattern was triangular and had a 70% infill factor.

The specimen pores will tend to produce an “apparent” slowing effect on bulk velocities measured. This is expected to be due to the accumulation of scattered paths that will cause the wavefront to travel longer distances to the receiver (i.e. it is not a straight line from Tx to Rx). This will be a consideration when measuring the velocity of the 3D printed samples as reference blocks. More work needs to be conducted on the most appropriate printed materials and internal patterns. Whilst the current material was “convenient”, perhaps it may not be consistent enough to be used as a reference standard. Also, there are many patterns that can be used to make the partial fill and each pattern will potentially have a subtle effect on the measured velocity. Because of the nature of the particle motion set up by the transducers (especially in shear mode) the orientation of the pattern relative to the probe motion will probably also be a factor.

### 3 RESULTS

#### 3.1 Transducer calibrations

As described in the previous section, a total of 25 different calibration tests were performed with the test setup. Analogue bandpass filters were used initially to remove unwanted signals prior to analysis. The repeatability of the results between the tests to measure the consistency is presented in Figure 7. Note that between each of the tests, the setup was completely disassembled and reassembled again to assess the reproducibility.

The DPP transducer used as the transmitter was excited with one sinusoidal cycle of 50 kHz with 120 Volts peak to peak. While the DPP receiver signal was pre-amplified with 20 dB gain and passed through a 100 Hz high pass analog filter before recording the response on an oscilloscope.

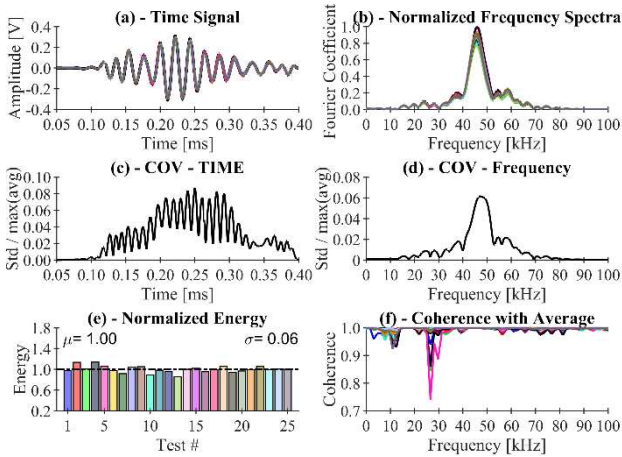


Figure 7. Statistical results measuring the repeatability of the tests.

Figure 7-a shows that the time signal of the different tests all overlap each other; the time signal is only shown for the first 0.4 ms of the response signal. The signal visually appears to be quite consistent. To measure the consistency, the standard deviation at each time step for all of the signals was computed and divided by the maximum absolute value on the time average of the signals (Figure 7-c). We are using the statistical measure of coefficient of variance (COV) because the main concept is to normalize the standard deviation with the average value. The maximum variation on the time signal amplitudes is around 8.7% and this variation occurs past the first wave arrival, around the peak of amplitudes of the first wave packet.

The frequency spectra for all of the time signals were also plotted for comparison in Figure 7-b. The computed spectra correspond only to the visible portion of the signal shown in Figure 7-a. The coefficient of variation was computed for the frequency spectra using the same procedure as for the COV on the time domain. The COV in the frequency domain follows a similar shape as the frequency spectra, with the highest variation around the main frequency peak with a value of 6.2% (see Figure 7-d).

The previous results show the degree of repeatability for the tests in terms of the signal shape and frequency content. To assess both simultaneously, the coefficient of coherence between each of the signals from each test and the average signal of all of them was computed and is shown in Figure 7-f. The plot shows the tests are coherent with themselves, with the major discrepancy around 25 kHz. However, this is not one of the predominant frequencies of the signal.

Finally, to measure the difference in attenuation of the signal between tests, the energy of the signal (area below the curve) for each of the tests was computed and normalized with the average value for all of them (Figure 7-e). The standard deviation of the normalized energy values is 6.4%.

The consistency results lack meaning without comparison of the consistency obtained with the transducer couple held by hand, instead of using the holder system. The same statistical analysis of the signals was performed on the signals obtained holding the transducers by hand. The coefficient of variation in time and frequency domain and the standard deviation for the normalized energy for both methods are compared in Figure 8.

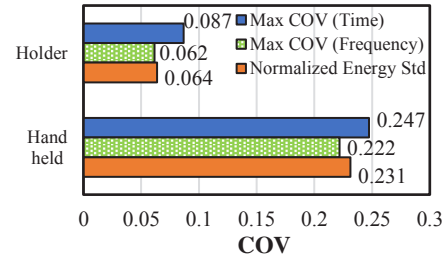


Figure 8. Comparison of the test consistency between the setup using the holders and hand holding the transducers.

### 4 DISCUSSION

As Figure 8 shows, the holder system that uses the spring and locking mechanism on the 3D printed calibration sample, reduces the variation of the signal between 2.7 and 3.6 times. The largest variability in both holding mechanisms occurs in the time domain. This could be due to slight changes in the trigger for recording the signals causing slight shifts in the phase of the signals. This explains the difference in the variation between the time and the frequency domain.

The large variation of ‘hand holding’ the transducer is expected due to lack of verticality while placing the transducer, misalignment of both transducers and changes in the contact pressure between transducer and sample. Higher repeatability could also be achieved by reducing the tolerance on the 3D printed parts, using more than 2 pins for the locking system to provide better lateral support.

### 5 CONCLUSIONS

A variation of the energy level of 6.4% is accurate enough to detect changes in attenuation of the material with time, and it is believed the variability can be further reduced. This paper has focused on the dry point transducer, however similar work is under development for the bender elements and P-wave transducers for the same system. The main challenge for the P-transducers is their large contact surface (compared with the single point of the dry point transducer) for which the same coupling conditions needs to be achieved. The coupling consistency for the bender elements is an even larger challenge, since it requires coupling on the tip, but also lateral coupling on the sides of the bender element. The coupling pressure also needs to be controlled to avoid buckling the tip. Trials of the ruggedized system are ongoing and further work is required to test these probes in an enhanced gravity environment in linear arrays, both in single and multiple modes of operation.

### 6 ACKNOWLEDGEMENTS

The authors would like to acknowledge the financial support of the Natural Sciences and Engineering Research Council (Grant: RGPIN-2015-06062) and the Canadian Foundation for Innovation (Grant: #33263).

### 7 REFERENCES

Abe, S., Kobayashi, Y. and Ikawa, T. 1990. Seismic characteristics of the weight-dropping source. *Journal of Physics of the Earth*. 38(3): 189-212.

- Aki, K. and Richards, P.G. 2002. *Quantitative seismology*. 2<sup>nd</sup> Edition University Science Books. pp. 704.
- Ali, H. 2015. *Study of Laboratory and Field Techniques to Measure Shear Wave Parameters-Frequency Effects*. PhD. Thesis University of Waterloo, Canada.
- Brandenberg, S.J., Choi, S., Kutter, B.L., Wilson, D.W. and Santamarina, J.C. 2006. A bender element system for measuring shear wave velocities in centrifuge models. In 6th *International Conference on Physical Modeling in Geotechnics*. 165-170.
- Camacho-Tauta, J., Jimenez Alvarez, J.D. and Reyes-Ortiz, O.J. 2012. A procedure to calibrate and perform the bender element test. *Dyna*. 79(176): 10-18.
- Chen, Y., Irfan, M., Uchimura, T., Wu, Y. and Yu, F. 2019. Development of elastic wave velocity threshold for rainfall-induced landslide prediction and early warning. *Landslides*. 16(5): 955-968.
- Cheney, J. A., Brown, R. K., Dhat, N. R. and Hor, O. 1990. Modeling free-field conditions in centrifuge models. *Journal of geotechnical engineering*. 116(9): 1347-1367.
- Coe, C.J., Prevost, J.H. and Scanlan, R.H. 1985. Dynamic stress wave reflections/attenuation: earthquake simulation in centrifuge soil models. *Earthquake engineering & structural dynamics*. 13(1): 109-128.
- Davies, M.C.R. 1994. Dynamic soil structure interaction resulting from blast loading. In *International conference centrifuge 94*. 319-324.
- Dyvik, R. and Madshus, C. 1985. Lab Measurements of  $G_m$  a x Using Bender Elements. In *Advances in the art of testing soils under cyclic conditions ASCE*. 186-196.
- Fu, L. 2004. *Application of piezoelectric sensors in soil property determination*. PhD. Thesis, Case Western Reserve University, USA.
- Garnier, J., Gaudin, C., Springman, S.M., Culligan, P.J., Goodings, D., Konig, D., Kutter, B., Phillips, R., Randolph, M.F. and Thorel, L. 2007. Catalogue of scaling laws and similitude questions in geotechnical centrifuge modelling. *International Journal of Physical Modelling in Geotechnics*. 7(3): 1-23.
- Itoh, K., Zeng, X., Koda, M., Murata, O. and Kusakabe, O. 2005. Centrifuge simulation of wave propagation due to vertical vibration on shallow foundations and vibration attenuation countermeasures. *Journal of Vibration and control*. 11(6): 781-800.
- Kırlangıç, A.S., Cascante, G. and Polak, M.A. 2015. Condition assessment of cementitious materials using surface waves in ultrasonic frequency range. *Geotechnical Testing Journal*. 38(2): 139-149.
- Lee, J.S. and Santamarina, J.C. 2005. Bender elements: performance and signal interpretation. *Journal of geotechnical and geoenvironmental engineering*. 131(9): 1063-1070.
- Lings, M.L. and Greening, P.D. 2001. A novel bender/extender element for soil testing. *Géotechnique*. 51(8): 713-717.
- Luong, M.P. 1994. Efficiency of a stress-wave mitigation barrier. In *International conference centrifuge 94* (pp. 283-288).
- Luong, P.M. 1994. Centrifuge simulation of Rayleigh waves in soils using a drop-ball arrangement. In *Dynamic Geotechnical Testing II*. ASTM International.
- Park, C.B., Miller, R.D. and Xia, J. 1997. Multi-channel analysis of surface waves (MASW)—a summary report of technical aspects, experimental results, and perspective. *Kansas Geological Survey*. 97-101.
- Park, C.B., Miller, R.D., Xia, J. and Ivanov, J. 2007. Multichannel analysis of surface waves (MASW)—active and passive methods. *The Leading Edge*. 26(1): 60-64.
- Rammah, K.I., Ismail, M.A. and Fahey, M. 2006. Development of a centrifuge seismic tomography system at UWA. In 6th *International Conference on Physical Modeling in Geotechnics*. 229-234.
- Semblat, J.F. and Luong, M.P. 1998. Wave propagation through soils in centrifuge testing. *Journal of earthquake engineering*. 2(01): 147-171.
- Shevaldykin, V., Samokrutov, A. and Kozlov, V. 2003. Ultrasonic Low-Frequency Short-Pulse Transducers with Dry Point Contact - Development and Application. In *Non-Destructive Testing in Civil Engineering 2003 - International Symposium (NDT-CE 2003)*.
- Taylor, R.N. 1995. *Geotechnical centrifuge technology*. CRC Press. pp. 296.
- White, D., Take, A. and Bolton, M. 2001. Measuring soil deformation in geotechnical models using digital images and PIV analysis. In 10th *International Conference on Computer Methods and Advances in Geomechanics*. Tucson, Arizona. 997-1002.